more conservatively. Unfortunately, the optimum long range strategy lies between 800 and 850 points per day which is too little to win a short contest. Basically, to win a championship, whether it be regional or national, a pilot must take risks in excess of optimum long range strategy and have a little luck. The crucial assumption here is that all pilots are equally capable, but that there is an even distribution of conservatism and rashness expressed by a speed-ring setting. In reality, there are many different levels of ability in any single contest and no one flies 80 knots all the way into the ground. Nevertheless in some diluted form, it is felt that the conclusion is valid. One must push and be a little lucky in order to win. The shorter the contest, the harder one must push.

A GENERAL METHOD FOR THE LAYOUT OF AILERONS AND ELEVATORS OF GLIDERS AND MOTORPLANES

Manfred Hiller
Institute A for Mechanics
University of Stuttgart

SUMMARY

A method is described which allows the layout of the spatial driving mechanism of the aileron for a glider or a motorplane to be performed in a systematic manner. In particular, a prescribed input-output behaviour of the mechanism can be realized by variation of individual parameters of the spatial four-bar mechanisms which constitute the entire driving mechanism. By means of a sensitivity analysis, a systematic choice of parameters is possible. At the same time the forces acting in the mechanism can be limited by imposing maximum values of the forces as secondary conditions during the variation process.

INTRODUCTION

The driving mechanism of the aileron and of the elevator of a glider or a motorplane is realized by a series-connection of spatial four-bar mechanisms, which transfer the movement of the control stick into the movement of the aileron. Generally, the relation between the movements is nonlinear. In the past, the layout of driving mechanisms has been performed mostly by means of the well known graphical techniques for plane mechanisms, treating parts of the spatial mechanism as plane problems. Today, as the driving mechanisms are getting more and more complicated, these techniques are no longer providing satisfying results (refs. 1 and 2).

Replacing the graphical techniques by a numerical method for the optimal layout of spatial transfer mechanisms, a given design can be modified in the desired way. The individual spatial four-bar mechanisms of the train are regarded as transfer elements, which can be treated separately. By means of a steepest descent method, the angular displacement of the tick and the aileron can be adjusted iteratively to a prescribed input-output behaviour. Thereby, individual parameters have to be chosen for variation (ref. 3).

The proposed method has been applied successfully to the layout of the driving mechanism of the aileron for the experimental glider fs-29*, with the desired differentiation of the displacement of the aileron. Two main experi-

* fs-29, an experimental glider with variable wing geometry, developed by the Akademische Fliegergruppe, University of Stuttgart, 1975.

ences showed that some improvements of the method are still necessary:

1. During the variation process, the loads acting in the mechanism may exceed maximum values, particularly if somewhere in the train for a certain position the angle between a crank and the corresponding coupler is either close to zero or close to 180 degrees. Considering prescribed maximum values of the loads as secondary conditions during the variation process, the acting loads can be limited.

2. Primarily, the choice of the parameters to be varied is arbitrary. Submitting the initial values of the geometrical data of the mechanism to a sensitivity analysis, a more systematic choice of the parameters is possible.

OPTIMAL LAYOUT OF SERIES-CONNECTED SPATIAL FOUR-BAR MECHANISMS

In a train of p series-connected spatial four-bar mechanisms, a single spatial four-bar mechanism consists of two rigid cranks $\underline{r}$ and $\underline{s}$ with skew-lying axes of rotation $\underline{u}$ and $\underline{w}$, and of the coupler $\underline{d}$, which is hinged to the cranks (figure 1). The bottoms of the vectors $\underline{r}$ and $\underline{s}$ are connected by the vector $\underline{\ell}$. The whole system has only one degree of freedom, and a rotation of the input-crank $\underline{r}$ about an input-angle β produces a unique rotation of the output-crank $\underline{s}$ about the output-angle γ. The rotations of the cranks $\underline{r}$ and $\underline{s}$ can be described by the pairs

$$(\underline{u},\beta) \tag{1}$$

$$(\underline{w},\gamma) \tag{2}$$

consisting of the vectors which describe the axes of rotation, and of the rotation angles. With respect to an initial position $\underline{r}_0$, $\underline{s}_0$ for the rotations of the cranks $\underline{r}$ and $\underline{s}$, the following homogeneous vector functions are valid:

$$\underline{r} = T(\underline{u},\beta)\underline{r}_0 \tag{3}$$

$$\underline{s} = U(\underline{w},\gamma)\underline{s}_0 \tag{4}$$

where $T(\underline{u},\beta)$ and $U(\underline{w},\gamma)$ are the tensors of rotations:

$$T(\underline{u},\beta) = \cos\beta\ I + (1-\cos\beta)\underline{u}\underline{o}\underline{u} + \sin\beta\ C \tag{5}$$

$$U(\underline{w},\gamma) = \cos\gamma\ I + (1-\cos\gamma)\underline{w}\underline{o}\underline{w} + \sin\gamma\ D \tag{6}$$

Here, I is the unit matrix, $\underline{u}\underline{o}\underline{u}$ and $\underline{w}\underline{o}\underline{w}$ are the dyadic products of the axis-vectors, while the skew-symmetric matrices C and D are composed by the axis-vectors $\underline{u}$ and $\underline{w}$. The unchangeable length of the coupler

$$\underline{d}^2 = \underline{d}_0^2 \tag{7}$$

yields the following algebraic equation for the output-angle γ :

$$a\cos\gamma + b\sin\gamma = c \tag{8}$$

with

$$a = (\underline{\ell}-\underline{r})^T(I-\underline{w}\underline{o}\underline{w})\underline{s}_0 \tag{9}$$

$$b = (\underline{\ell}-\underline{r})^T D\underline{s}_0 \tag{10}$$

$$c = a - (\underline{s}_0+\underline{\ell})^T(\underline{r}_0-\underline{r}) \tag{11}$$

Therefore, the output-angle γ is a nonlinear function of the input-angle β, and of the describing vectors $\underline{u}$, $\underline{r}$, $\underline{\ell}$, $\underline{w}$, $\underline{s}$:

$$\gamma = f(\beta,\underline{u},\underline{r},\underline{\ell},\underline{w},\underline{s}) \tag{12}$$

By a series-connection of several spatial four-bar mechanisms, a spatial transfer mechanism is realized (figure 2). The j-th four-bar mechanism is described by the vectors

$$\underline{u}_j,\ \underline{r}_j,\ \underline{\ell}_j,\ \underline{w}_j,\ \underline{s}_j \qquad j = 1,\ldots,p \tag{13}$$

and by the following correspondence of angles

$$\gamma_j = \beta_{j+1} \qquad j = 1,\ldots,p \tag{14}$$

The output-angle γ_j is a nonlinear function of the input-angle β_1 and of the vectors given by equation (13):

$$\gamma_j = f(\beta_1, \underline{u}_i, \underline{r}_i, \underline{\ell}_i, \underline{w}_i, \underline{s}_i) \qquad \begin{matrix} i = 1,\ldots,j \\ j = 1,\ldots,p \end{matrix} \tag{15}$$

By variation of a set of arbitrary chosen components of the vectors $\underline{u}_j$, $\underline{r}_j$, $\underline{\ell}_j$, $\underline{w}_j$, $\underline{s}_j$, the input-output behaviour of the kinematical train can be changed in such a way that to a given number of m input-angle positions β_1, the output-angles γ_j can be adjusted to prescribed values γ_{sj}. The variation of the parameters follows from a steepest descent method, minimizing iteratively the least-squares error

$$[\underline{y}(\underline{x})-\underline{y}_s]^T[\underline{y}(\underline{x})-\underline{y}_s] \tag{16}$$

where the set of parameters is summarized in the parameter-vector $\underline{x}$ of dimension n, the prescribed output-angles in the nominal-value vector $\underline{y}_s$ of dimension m, and the actual output-angles are summarized in the vector $\underline{y}$.

Due to the r-th iteration step, we have an improvement of the parameter-vector $\underline{x}^{(r-1)}$

$$\underline{x}^{(r)} = \underline{x}^{(r-1)} + \underline{\xi}^{(r)} \tag{17}$$

where the improvement $\underline{\xi}^{(r)}$ is given by the solution of the algebraic equation

$$A^{(r-1)T}A^{(r-1)}\underline{\xi}^{(r)} + A^{(r-1)T}\underline{d}^{(r-1)} = \underline{0} \tag{18}$$

Here, $A^{(r-1)}$ is the Jacobian matrix of partial derivatives of the nominal-value vector with respect to the parameter-vector, during the r-th iteration step. For the vector $\underline{d}^{(r-1)}$,

$$\underline{d}^{(r-1)} = \underline{y}^{(r-1)} - \underline{y}_s \tag{19}$$

The proposed method enables an optimal adjustment of the actual output-angles to the set of prescribed nominal values with respect to the least-squares error, with only few iteration steps necessary for convergence. To make the iteration method applicable, a set of kinematically compatible data at the beginning of the iteration process is required.

EXTENDED METHOD CONSIDERING MAXIMUM LOADS AS SECONDARY CONDITIONS

Regarding only slow motions of the transfer mechanism, the inertial forces of the system may be neglected, and the loads acting in the hinges and the bearings can be calculated statically. Furthermore, in real systems the dead loads of the cranks and the couplers may be neglected, because they are small in comparison to the acting forces. The hinged articulations between the cranks and the couplers are regarded as ideal constraints, and consequently the coupler forces are directed along the coupler itself.

Cutting the j-th four-bar mechanism in a train of p series-connected spatial four-bar mechanisms, the coupler force of the preceding four-bar mechanism acts as an input-load, whereas the output-load is the coupler force of the succeeding four-bar mechanism. Thus, we have a propagating flux of forces passing through the whole train (figure 3). For the coupler force of the j-th four-bar mechanism, we obtain

$$\underline{f}_{r,j} = \frac{\underline{f}_{s,j-1}}{\underline{d}_{j-1}} \frac{(\underline{s}_{j-1} \times \underline{d}_{j-1}) \cdot \underline{w}_{j-1}}{(\underline{d}_j \times \underline{r}_j) \cdot \underline{u}_j} \underline{d}_j \tag{20}$$

which is a function of the coupler force of the preceding four-bar mechanism, and of the geometrical data of the (j-1)-th and the j-th four-bar mechanism, respectively (see ref. 4). From equation (20) it follows that according to the numerator, the geometry of the preceding four-bar mechanism is responsible for the zeros of the coupler force, while the geometry of the regarded four-bar mechanism is responsible for the poles of the coupler force, according to the denominator.

The engineering design of a spatial transfer mechanism is often characterized by prescribed constraints, which can be either geometrical boundaries due to limitations in the available space, or which can be restrictions for the permissible loads in the mechanism. During the iteration process, these constraints may be violated, due to the variation of the parameters. Considering the constraints as secondary conditions in the iteration method, this can be avoided. In case of permissible loads, the corresponding secondary conditions are inequalities which have to be considered in a specific way. In the following, the restriction of the coupler force which is of most importance will be discussed in more detail.

Generally, the coupler force, designated as $\underline{f}_j$, is a nonlinear function of the input-angle β_1, and of the describing vectors of the four-bar mechanisms, according to equation(20):

$$\underline{f}_j = \underline{f}_j(\beta_1, \underline{u}_i, \underline{r}_i, \underline{s}_i, \underline{w}_i, \underline{s}_i) \qquad \begin{matrix} i = 1,\ldots,j \\ j = 1,\ldots,p \end{matrix} \tag{21}$$

During the iteration process, the coupler forces will change, due to the variation of the designated parameters. If the residual components of the describing vectors are regarded to be constant, the coupler force depends only on the input-angle β_1 , and on the parameter-vector $\underline{x}$:

$$\underline{f}_j = \underline{f}_j(\beta_1, \underline{x}) \qquad j = 1,\ldots,p \tag{22}$$

Now, it may happen that individual coupler forces exceed maximum values for certain positions of the train, particularly if somewhere in the train the angle between a crank and the corresponding coupler is either close to zero or close to 180 degrees. Thereby, only the magnitude of the coupler force is of interest, for its direction is given by the direction of the coupler. Furthermore, compressive forces are more important than tension forces. If f_{jo} is the permissible value of the j-th coupler force, the difference between the actual and the permissible force is given by

$$g_j(\beta_1, \underline{x}) = f_j(\beta_1, \underline{x}) - f_{jo} \qquad j = 1,\ldots,p \tag{23}$$

and the following secondary condition is valid:

$$g_j(\beta_1, \underline{x}) \leq 0 \qquad j = 1,\ldots,p \tag{24}$$

Hence, the iteration method may be split into two parts. As long as equation (24) is not violated, the iteration process operates in the way described above. The r-th iteration step is given by equation (17):

$$\underline{x}^{(r)} = \underline{x}^{(r-1)} + \underline{\xi}^{(r)}$$

If equation (24) is violated during the r-th iteration step for at least one index j (input-angle β_1 fixed), we have

$$g_j(\beta_1, \underline{x}) > 0 \qquad j \in \{1,\ldots,p\} \tag{25}$$

Consequently, the parameter-vector $\underline{x}^{(r)}$ has to be corrected. In a first step, the intersection point $\underline{x}_s$ of the corrective vector $\underline{\xi}^{(r)}$ with the surface of separation $g_j(\beta_1, \underline{x})=0$ has to be determined. In a second step, the vector $\underline{\xi}^{(r)}$ can be separated in two components:

$$\underline{\xi}_1^{(r)} = \underline{x}_s - \underline{x}^{(r-1)} \tag{26}$$

$$\underline{\xi}_2^{(r)} = \underline{x}^{(r)} - \underline{x}_s \tag{27}$$

Then, the component $\underline{\xi}_2^{(r)}$ has to be projected into the tangential plane of the surface $g_j(\beta_1,\underline{x})=0$, at point $\underline{x}_s$. Thus, we have the new corrective vector for the r-th iteration step (figure 4):

$$\underline{x}'^{(r)} = \underline{x}^{(r-1)} + \underline{\xi}_1^{(r)} + \underline{\xi}_{2t}^{(r)} \tag{28}$$

which is the most favorable correction referring to the secondary condition (24). If

$$g_j(\beta_1,\underline{x}'^{(r)}) < 0 \qquad j = 1,\ldots,p \tag{29}$$

the iteration process continues with the next step. If, on the other hand

$$g_j(\beta_1,\underline{x}'^{(r)}) > 0 \qquad j \in \{1,\ldots,p\} \tag{30}$$

the vector $\underline{x}'^{(r)}$ has to be corrected again. Starting from point $\underline{x}'^{(r)}$, and proceeding against the gradient $\partial g_j(\beta_1,\underline{x})/\partial\underline{x}$, we arrive after the second correction at point $\underline{x}''^{(r)}$, for which

$$g_j(\beta_1,\underline{x}''^{(r)}) \leq 0 \qquad j = 1,\ldots,p \tag{31}$$

is valid (figure 5), and the iteration process will be continued with the next step. By means of the described correcting procedure, the variation of the parameter-vector $\underline{x}$ occurs in the neighbourhood of the surface of separation

$$g_j(\beta_1,\underline{x}) = 0 \qquad j = 1,\ldots,p \tag{32}$$

if the secondary condition (24) is violated. Until now, the input-angle β_1 was assumed to be fixed. Actually, we have an assignment of m input-angles β_1 to m prescribed output-angles γ_j, and consequently, the secondary condition (24) has to be checked for every input-angle position β_1. In practical cases, the coupler forces will exceed their maximum values only for small domains of angular positions, due to the kinematical reasons mentioned above, so that the secondary condition (24) has to be examined only for individual angular positions.

PARAMETER SENSITIVITY AND CHOICE OF PARAMETERS

Primarily, the choice of the set of parameters for the iteration process is arbitrary. In practical applications, one difficulty arises from the questions, which parameters shall be chosen, and how many parameters shall be varied? As each component of the five vectors

$$\underline{u}_j, \underline{r}_j, \underline{\ell}_j, \underline{w}_j, \underline{s}_j$$

which describe a spatial four-bar mechanism, may serve as parameters, we have a set of 15 available parameters for every four-bar mechanism. Accordingly, the number of parameters increases in a train of series-connected four-bar mechanisms. By means of a systematic sensitivity analysis applied to the initial data of the train, before starting the iteration, it is possible to get some information about the kinematical behaviour with respect to variations of individual components of the vectors involved.

Designating the indicated four-bar mechanism with index-number j_o, where the changed vectors are

$$\hat{\underline{u}}_{jo}, \hat{\underline{r}}_{jo}, \hat{\underline{\ell}}_{jo}, \hat{\underline{w}}_{jo}, \hat{\underline{s}}_{jo} \tag{33}$$

the output-angles of the train are given on the one hand by

$$\gamma_j = f(\beta_1, \underline{u}_i, \underline{r}_i, \underline{\ell}_i, \underline{w}_i, \underline{s}_i) \qquad \begin{matrix} i = 1,\ldots,j \\ j = 1,\ldots,j_o-1 \end{matrix} \tag{34}$$

and on the other hand by the new values

$$\hat{\gamma}_{jo} = f(\beta_1, \hat{\underline{u}}_{jo}, \hat{\underline{r}}_{jo}, \hat{\underline{\ell}}_{jo}, \hat{\underline{w}}_{jo}, \hat{\underline{s}}_{jo}) \tag{35}$$

$$\hat{\gamma}_j = f(\beta_1, \underline{u}_i, \underline{r}_i, \underline{\ell}_i, \underline{w}_i, \underline{s}_i) \qquad \begin{matrix} i = j_o+1,\ldots,j \\ j = j_o+1,\ldots,p \end{matrix} \tag{36}$$

Thus, the changed vectors (equation (33)) are not only influencing the transfer behaviour of the four-bar mechanism with index-number j_o, but also the behaviour of all subsequent four-bar mechanisms, while the preceding four-bar mechanisms remain unchanged.

The difference

$$\Delta\gamma_j = \hat{\gamma}_j - \gamma_j \qquad j = j_o,\ldots,p \tag{37}$$

serves as a measure for the sensitivity of the transfer behaviour of the kinematical train against changes in its vectors.

For a complete sensitivity analysis, it is necessary to examine the influence of the individual components separately. Moreover, the vector components have to be changed in the same way, to enable the comparison between different sensitivities. Among the different possibilities of changing the vector components, the method where the ratio of change remains constant has proved to be the most successful. If in a certain vector one component is equal to zero, another component which is not equal to zero serves as reference value. The difference angle $\Delta\gamma_j$ is plotted versus the input-angle β_1, and for the j-th and all subsequent four-bar mechanisms we have a family of 15 curves each, which are representing the sensitivity of the j-th four-bar mechanism. By means of the plotted curves, a more systematic choice of the parameters for the variation process is possible.

The sensitivity analysis has been performed on the basis of the initial data of the kinematical train. During the iteration process, the sensitivities of the selected parameters, as well as the sensitivities of the residual components involved will change, because of their nonlinear interdependence. Therefore, it is suitable to subject the whole system to another sensitivity analysis at the end of the iteration process. It might also be taken into consideration to control the sensitivity of the system during the iteration process, but the required numerical effort is considerable.

The advantages of the proposed sensitivity analysis consist not only in a more systematic choice of parameters for the optimal layout of the transfer mechanism, but at the same time it enables an estimation of the deviations in the transfer behaviour, which arise from manufacturing defects or from bearing play in the hinges.

PROGRAM SYSTEM

For application, a sophisticated and user-oriented program system has been developed, the more important aspects of which are:

1. The determination of the kinematical transfer behaviour and of the range of kinematical compatibility of the train, by a stepwise change of the input-angle β_1.

2. The determination of the transfer behaviour of the coupler forces for a given input load, by a stepwise change of the input-angle β_1.

3. The determination of the output-angles and of the coupler forces, as well as the influences caused by the changes of parameters.

4. A systematic analysis of the individual four-bar mechanisms, concerning domains of kinematical compatibility and poles in the coupler forces, as well as angular positions, for which the train becomes unstable.

5. A systematic sensitivity analysis of the kinematical train, which enables on the one side a systematic choice of parameters for variation, and which provides on the other side information about the influence of inaccuracies on the transfer behaviour of the train.

APPLICATIONS

In the following, the application of the described method to the driving mechanism of the aileron for the glider fs-29 will be discussed in more detail. The fs-29 is an experimental glider developed at the University of Stuttgart. Due to telescoping wings, the wing span of the glider can be varied during flight. The driving mechanism of the aileron consists of 10 series-connected spatial four-bar mechanisms. By means of the variation method in its original version, the driving mechanism has been laid out successfully, assigning desired aileron deflections to given stick positions. But a large number of computer runs were necessary, trying various sets of parameters (consisting of 2 or 3 parameters). The parameters were components of the cranks $\underline{r}_j$ and $\underline{s}_j$ in the neighbourhood of the aileron. Flight tests showed that for certain positions of the mechanism the coupler forces exceeded permissible values. By application of the extended variation method, these disadvantages can be avoided.

The numbering of the series-connected four-bar mechanisms starts with the stick, as the input-movement of the stick produces the output-movement of the aileron. Table 1 shows the initial data of the driving mechanism (all distances in meters). The data of the involved four-bar mechanisms (except the four-bar mechanisms 8, 9, 10) are given in the same cartesian coordinate system: x-axis ≙ axis of pitch, y-axis ≙ axis of yaw, z-axis ≙ axis of roll. The required four assignments of stick position to aileron deflection are shown in table 2. The transfer behaviour of the coupler forces will be tested by a unit input-load acting on the stick. Figure 6 and figure 7 show the input-output behaviour of the individual four-bar mechanisms as a function of the stick deflection β_1. Before starting the variation process, a sensitivity analysis for the four-bar mechanisms 7, 8, 9, and 10 has been performed. The sensitivities of the cranks $\underline{r}_9$, $\underline{s}_9$, and $\underline{r}_{10}$, $\underline{s}_{10}$, respectively, are shown in figure 8 and figure 9. (The influence of $\underline{r}_9$, $\underline{s}_9$ on four-bar mechanism 10 is not displayed.) Satisfactory optimization results are obtained by combinations of parameters with high and low sensitivity, from which the parameter combina-

tion $r_{9,1}$, $r_{10,1}$ has been selected. Here, $r_{9,1}$ and $r_{10,1}$ are the x-components of the cranks $\underline{r}_9$ and $\underline{r}_{10}$, respectively.

The behaviour of the aileron deflection γ_{10} as a function of the stick position β_1 is shown in figure 11. The approximation of the prescribed values of table 2 is within an accuracy of 0.6 degrees. (The curve $\gamma_9(\beta_1)$ is given by figure 10.) Due to the variation process, the coupler force f_9 has completely changed its behaviour (see figure 12). However, the maximum values can be considerably reduced by prescribing maximum limiting values of the coupler forces as secondary conditions, as shown in figure 13. In this case, the accuracy of the required assignment is reduced, but still sufficient.

During flight, the input-output displacement propagates from the stick to the aileron, whereas, looking to the forces, the aerodynamic forces on the aileron are the input-loads, which have to be balanced by the pilot through the stick. In this case, the application of the variation method gets more complicated, because the transfer mechanism has to be investigated in both directions (see ref. 4). Figure 14 shows an example, where critical values of the coupler force in the seventh four-bar mechanism have been reduced. The input-load at the aileron has been the constant moment $\underline{m}_A = (23.34,0,0)$ [Nm] .

CONCLUSIONS

The layout of spatial transfer-mechanisms consisting of series-connected spatial four-bar mechanisms can be performed more effectively if the graphical techniques are replaced by a numerical method. Within this method, the individual four-bar mechanisms are treated analytically as transfer elements. By variation of selected parameters, the input-output behaviour of the train can be adjusted to prescribed values. The acting loads in the mechanism can be limited, considering maximum values of the loads as secondary conditions during the variation process. The effectiveness of the proposed method has been demonstrated at the layout of the driving mechanism for the aileron of a glider.

REFERENCES

1. Beyer, R.: Technische Kinematik. Ambrosius-Verlag, Leipzig, 1931.

2. Hall, A. S.: Kinematics and Linkage Design. Prentice-Hall, Englewood Cliffs, N.J., 1961.

3. Eppler, R.; Miller, M.: Numerische Behandlung von Gelenkvierecken mit vorgeschriebenem Ausgang. DLR-Forschungsbericht 75-[illegible], pp. 53-[illegible], 1975.

4. Miller, M.: Ein Verfahren zur optimalen Auslegung von mechanischen Ruderantrieben bei Segelflugzeugen und Motorsportflugzeugen. Zeitschrift für Flugwissenschaften und Weltraumforschung (ZFW), May 1979.

TABLE 1.- INITIAL DATA OF AILERON DRIVING MECHANISM

OF THE EXPERIMENTAL GLIDER, fs-29

four-bar mechanism	$\underline{r}_j$ [m]	$\underline{u}_j$	$\underline{\ell}_j$ [m]	$\underline{s}_j$ [m]	$\underline{w}_j$
1	0.0000 0.0430 0.0150	0.0000 -0.0190 0.2000	0.1250 0.0400 -0.0450	0.0000 -0.0062 0.0596	0.0000 -0.3875 -0.0400
2	0.0800 0.0000 0.0000	0.0000 -0.3875 -0.0400	0.0000 -0.0200 -0.8810	0.0000 0.0650 -0.0100	1.0000 0.0000 0.0000
3	0.0000 0.0610 -0.0210	1.0000 0.0000 0.0000	0.0000 -0.0960 -0.3820	0.0000 0.0580 0.0060	1.0000 0.0000 0.0000
4	0.0000 0.0400 -0.0430	1.0000 0.0000 0.0000	-0.0060 -0.2430 -0.1490	-0.0800 0.0000 0.0000	0.0000 0.0590 -0.1000
5	0.0000 -0.0690 -0.0400	0.0000 0.5900 -0.1000	3.0600 -0.0570 0.1120	0.0000 -0.0080 0.1350	0.0000 1.0000 0.0000
6	0.0900 -0.0070 -0.0665	0.0000 1.0000 0.0000	0.1150 -0.0510 -0.0090	-0.0250 0.0590 -0.0150	-1.0000 0.0000 0.0000
7	0.0000 0.0420 -0.0270	-1.0000 0.0000 0.0000	0.0000 0.0290 -0.0900	0.0000 -0.0125 0.0480	1.0000 0.0000 0.0000
8	0.0020 -0.0170 0.0470	0.0810 0.0000 -0.0030	-0.0480 0.0220 0.0510	0.0500 0.0000 -0.0015	-0.0030 0.0035 -0.0845
9	0.0220 -0.0490 0.0120	-0.0030 0.0000 -0.0835	0.5860 -0.0200 -0.0640	-0.0480 0.0280 0.0510	0.0000 -1.0000 0.0000
10	0.0400 0.0000 -0.0020	0.0000 1.0000 0.0000	0.0500 0.0400 -0.0740	0.0000 -0.0405 0.0045	-1.0000 0.0000 0.0000

TABLE 2.- INPUT/OUTPUT ANGULAR RELATIONSHIPS FOR STICK AND AILERON OF fs-29 GLIDER

input-angle at stick	β_1 [°]	-22.1	-12.7	14.1	26.4
output-angle at aileron	γ_{10} [°]	-25.0	-12.6	8.9	15.0

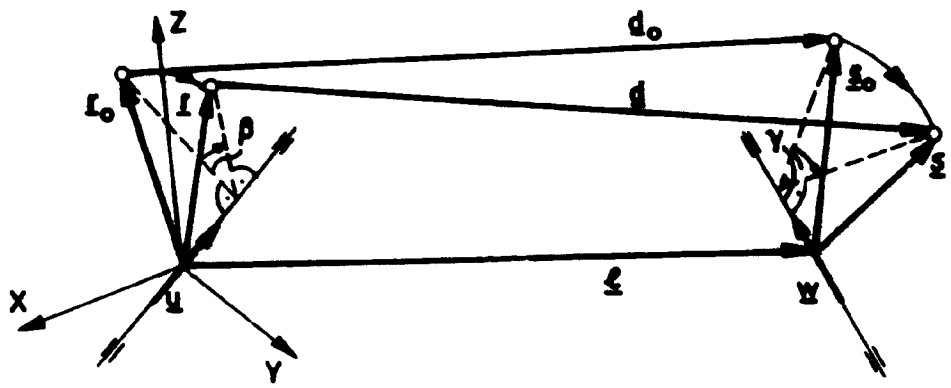

Figure 1: The spatial four-bar mechanism.

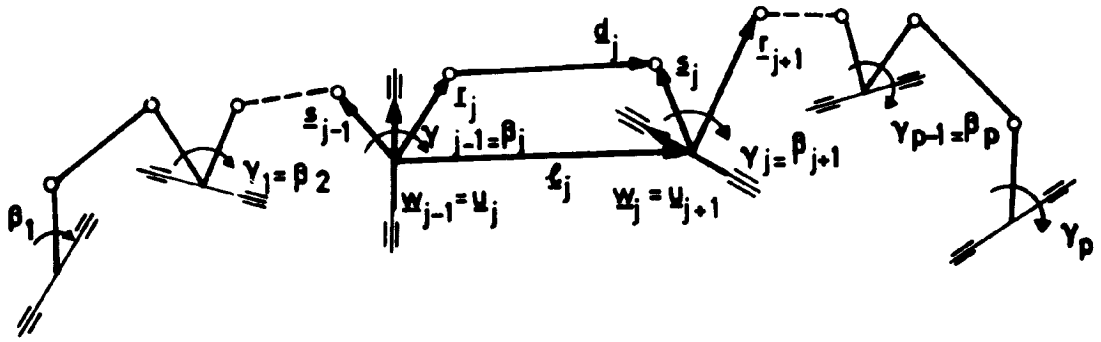

Figure 2: The spatial transfer mechanism.

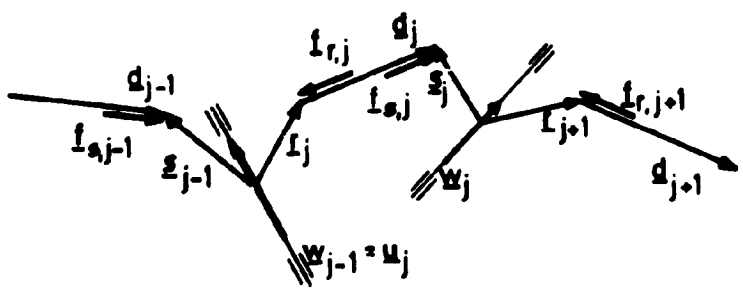

Figure 3: Coupler force.

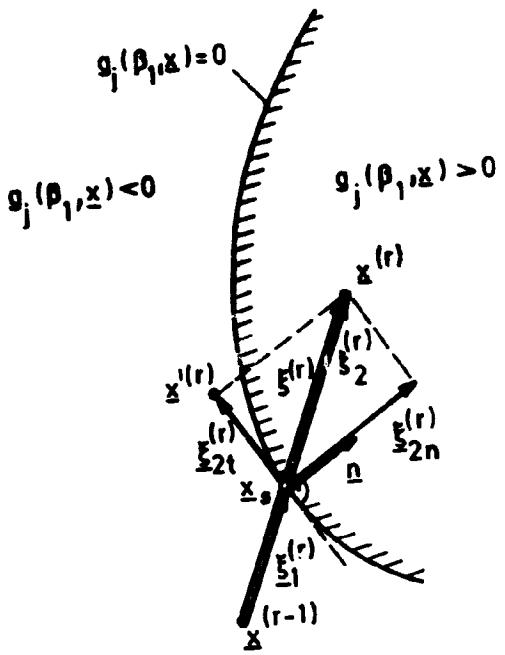

Figure 4: Correction step 1 for secondary condition.

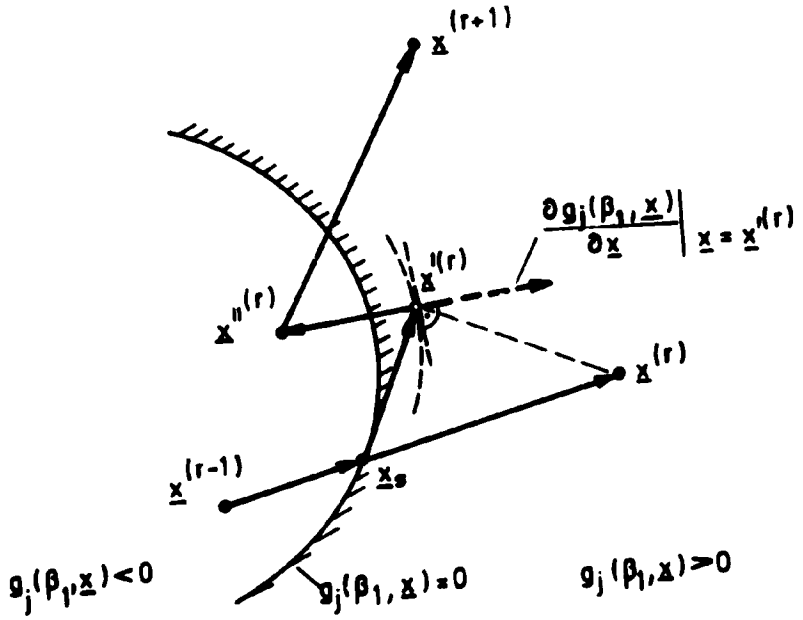

Figure 5: Correction step 2 for secondary condition.

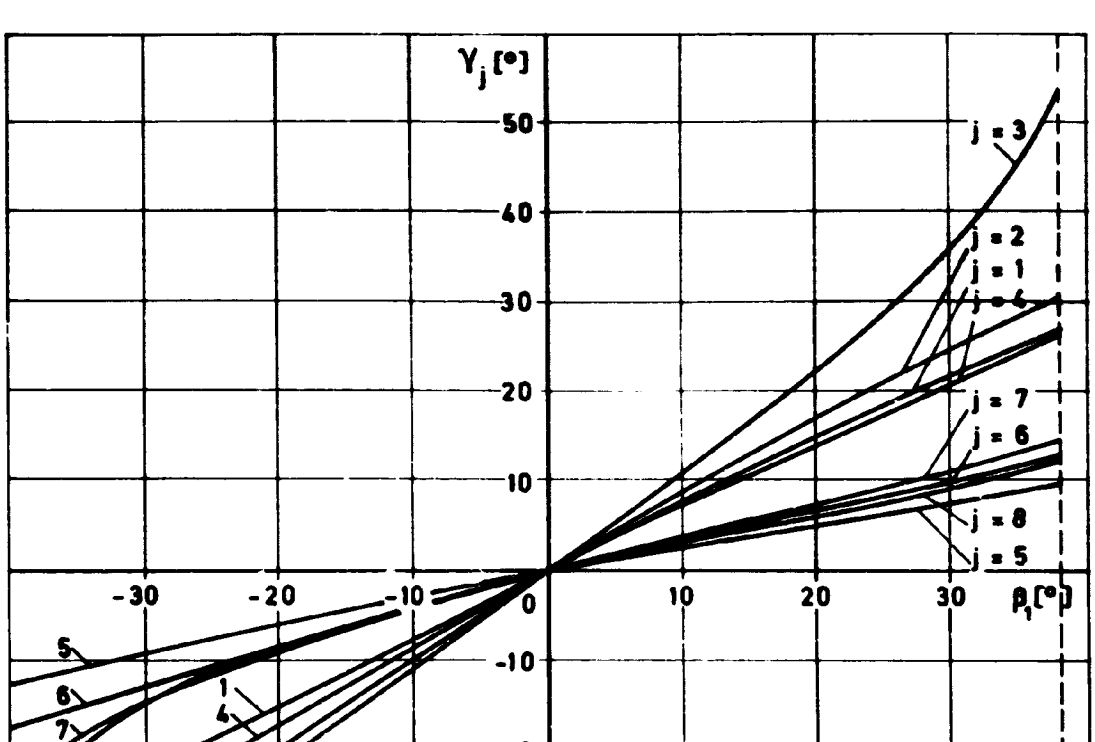

Figure 6: Input-output behaviour of four-bar mechanisms 1 to 8.

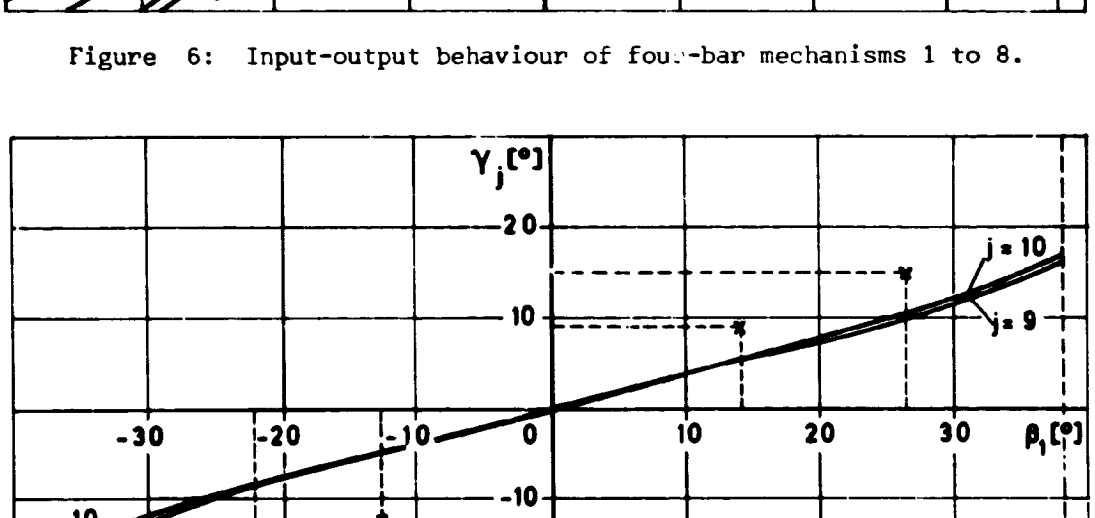

Figure 7: Input-output behaviour of four-bar mechanisms 9 and 10.

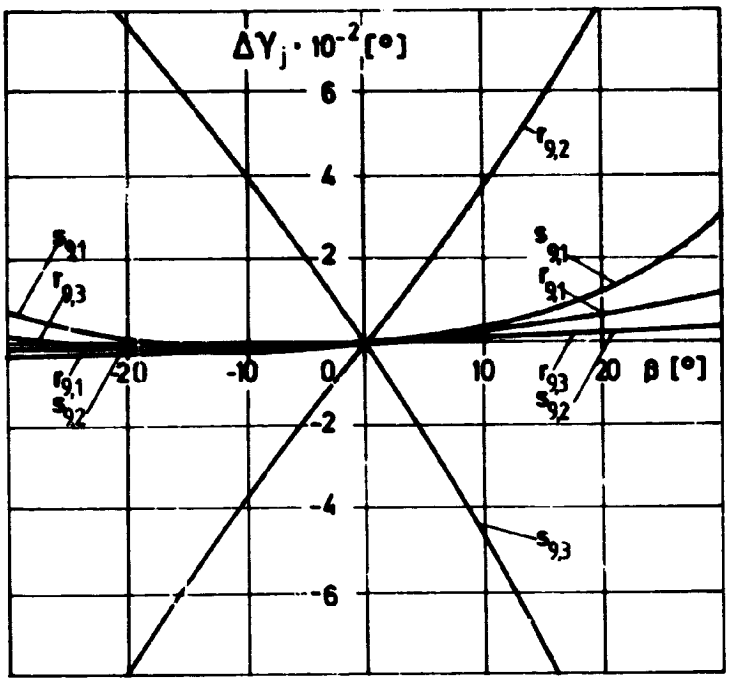

Figure 8: Sensitivity of the cranks $\underline{r}_9$ and $\underline{s}_9$.

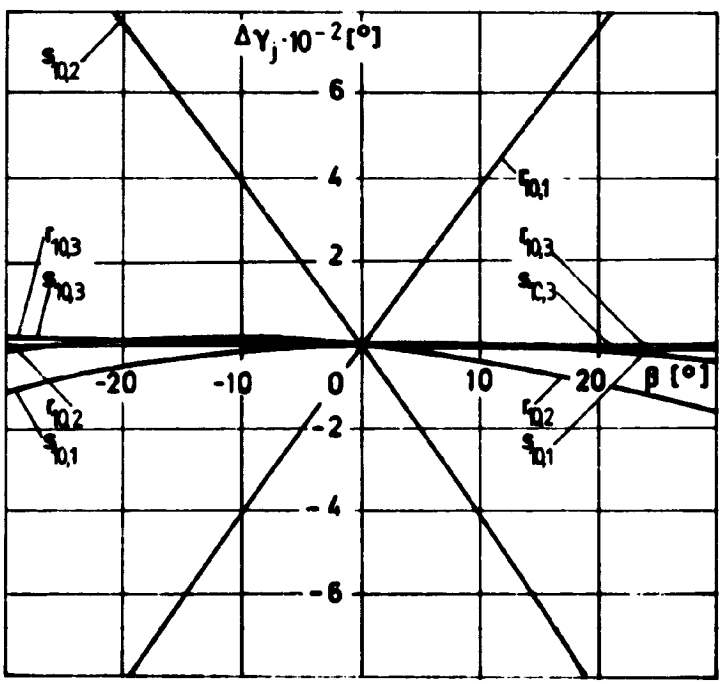

Figure 9: Sensitivity of the cranks $\underline{r}_{10}$ and $\underline{s}_{10}$.

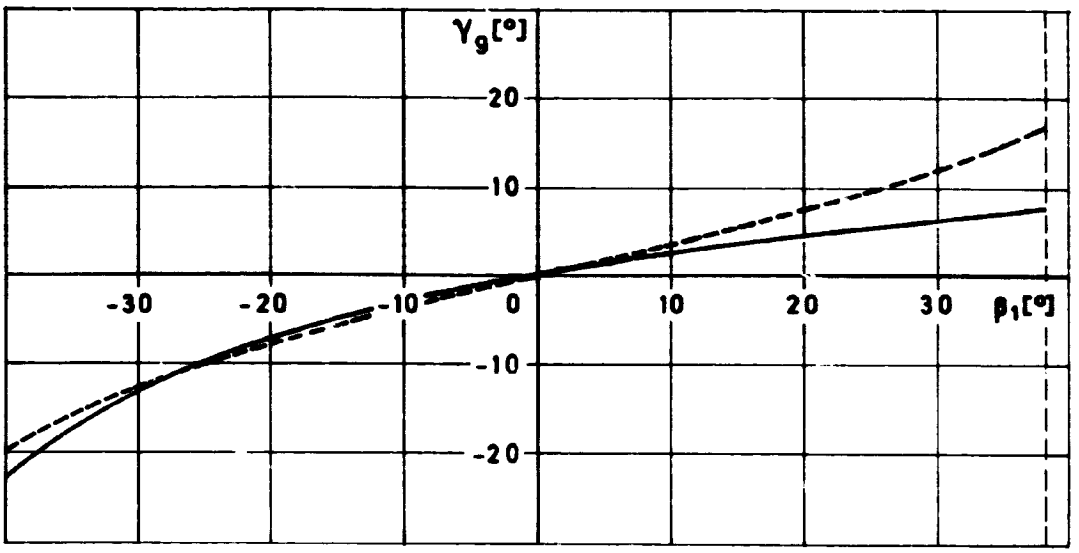

Figure 10: Output-angle γ_9 before (---) and after (——) variation.

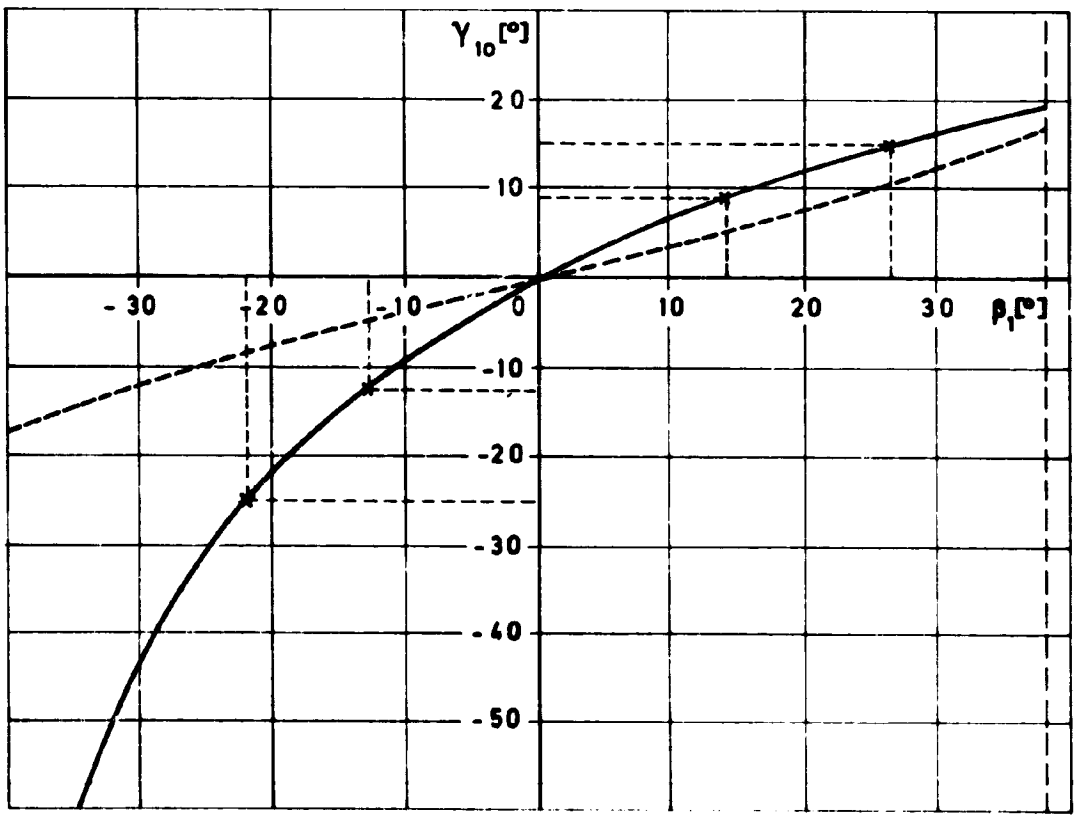

Figure 11: Aileron deflection γ_{10} before (---) and after (——) variation.

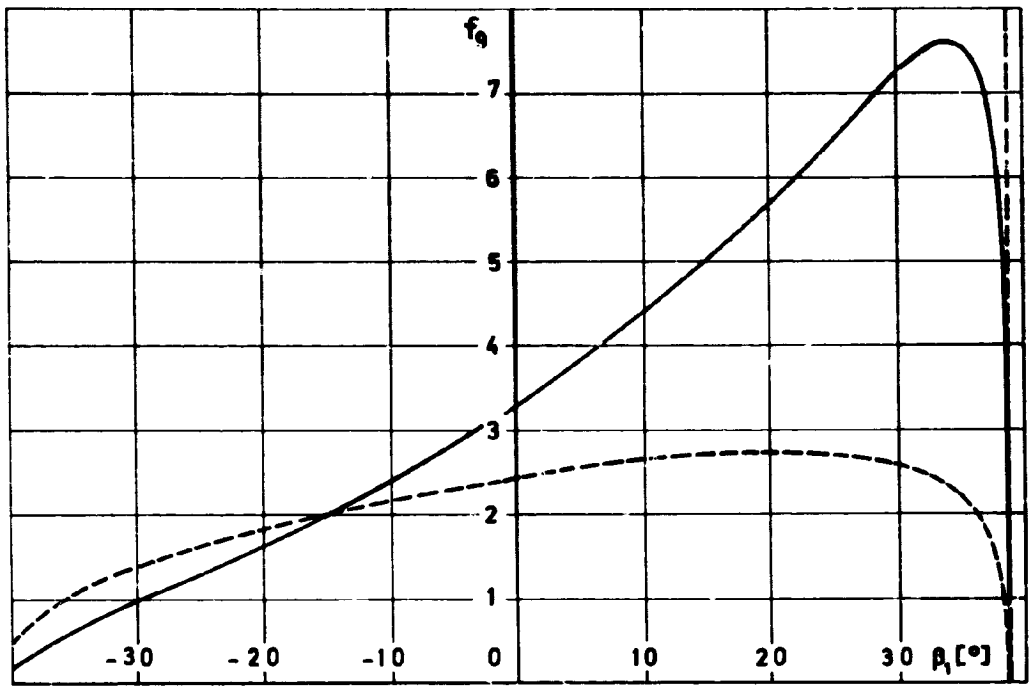

Figure 12: Coupler force f_9 before (– – –) and after (——) variation.

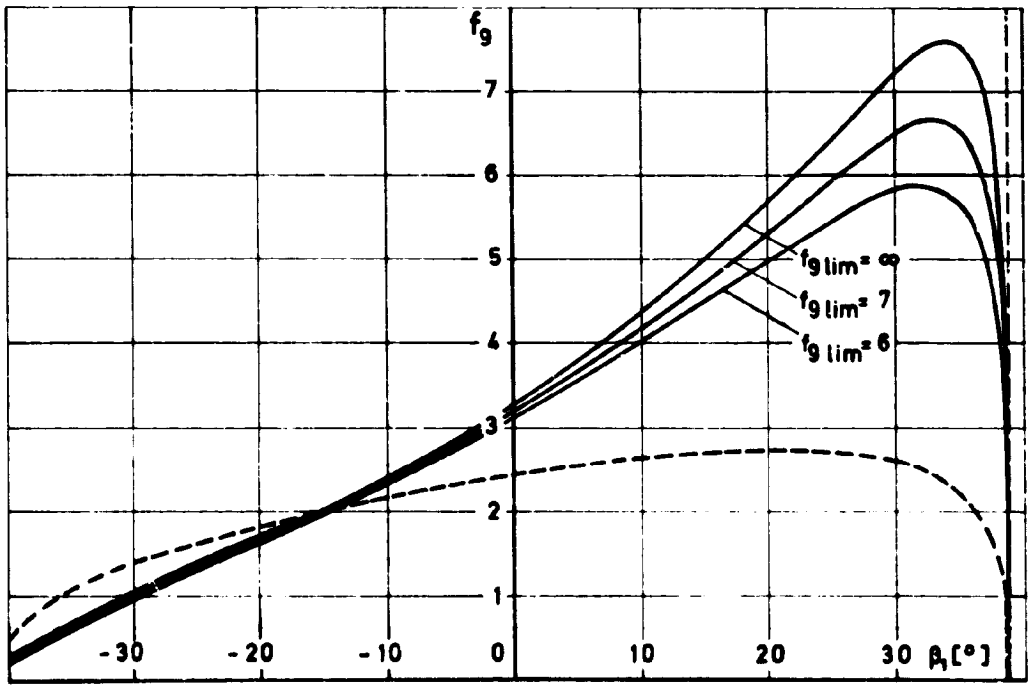

Figure 13: Limited coupler force f_9

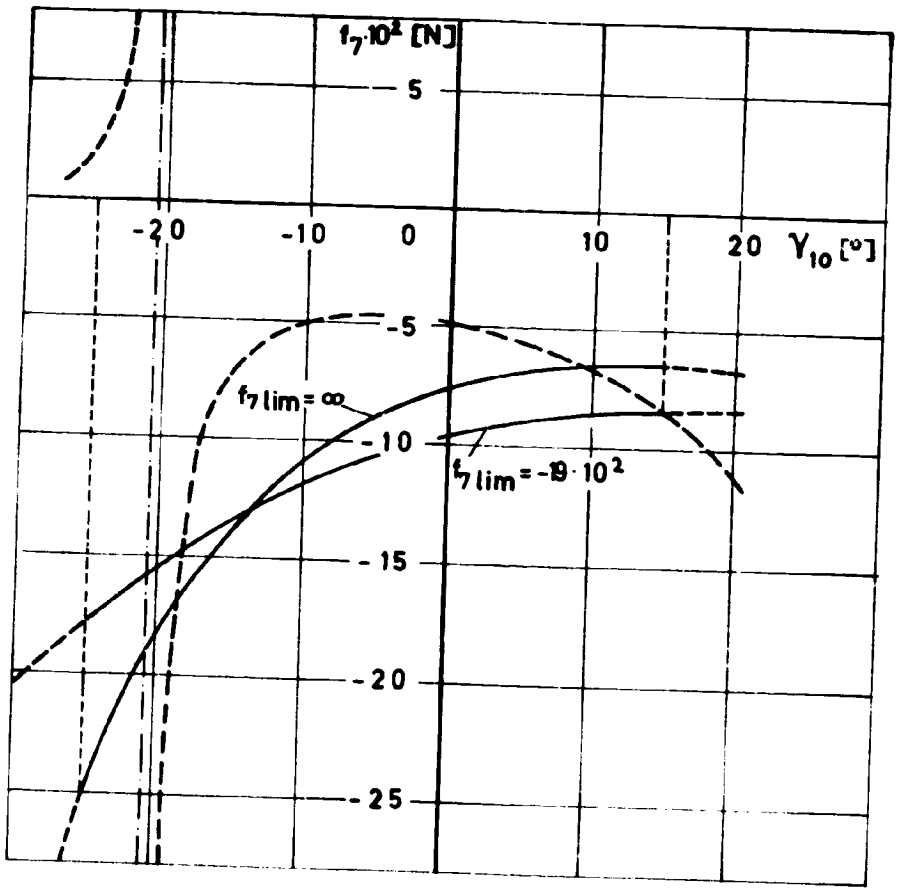

Figure 14: Coupler force f_7 before (– – –) and after (——) variation.

N79-27077

EXPERIMENTAL INVESTIGATION INTO THE FEASIBILITY OF AN "EXTRUDED" WING

Piero Morelli and Giulio Romeo
Politecnico di Torino, Italy

SUMMARY

Research work in the Politecnico di Torino and realizations (fabrications) of extruded aluminium alloy structures during the past years is briefly reviewed. The design criteria and the realization of the main structure of a sailplane wing made of a few extruded profiles longitudinally connected one to the other are then illustrated. Structural tests recently carried out are reported upon.

INTRODUCTION

Early research work and the first realizations on the M-300 sailplane prototypes were reported upon in reference 1. Figure 1 illustrates the cross section of the M-300 extruded structures: first and second realization of the ailerons (a,b), tailplane (c), wing spar (d). An aluminium alloy AlMgSi TA16 (A.A. 6063-T6) was employed for the extrusion except for the spar, which was of A.A.7075.

In more recent years the same structural concept was adopted by the firm Caproni Vizzola Costruzioni Aeronautiche, manufacturer of the two-seater sailplane Calif A-21S (ref.2 and 3). Figure 2 illustrates some of the parts of this glider which were realized by extrusion using the same aluminium alloy mentioned above: airbrake (a), flap (b), aileron (c), elevator (d), and leading edge of the wing central part (e). The aileron and elevator extruded profiles incorporate the hinge (A). In the aileron leading edge lodging is provided (B) for the counterweight, uniformly distributed along the span for static and dynamic balance.

In the M-300 and Calif extruded structures the original wall thickness of 1.8 to 2.0 mm was reduced to design values of .5 to .8 mm by chemical milling of the outer surface.

All these structures are basically ribless. They proved light and largely adequate in strength and stiffness.

One of the M-300 prototypes is still active. The Calif two-seater has been series produced with the extruded parts mentioned here since 1975, except the extruded airbrake which was introduced in 1978.